

Insights into the Mechanistic Dichotomy of the Protein Farnesyltransferase Peptide Substrates CVIM and CVLS

Yue Yang,[†] Bing Wang,[†] Melek N. Ucisik,[†] Guanglei Cui,[†] Carol A. Fierke,^{‡,*} and Kenneth M. Merz, Jr.*[†]

[†]Department of Chemistry and the Quantum Theory Project, 2328 New Physics Building, P.O. Box 118435, University of Florida, Gainesville, Florida 32611-8435, United States

[‡]Departments of Chemistry and Biological Chemistry, The University of Michigan, Ann Arbor, Michigan 48109-1055, United States

S Supporting Information

ABSTRACT: Protein farnesyltransferase (FTase) catalyzes farnesylation of a variety of peptide substrates. ³H α -secondary kinetic isotope effect (α -SKIE) measurements of two peptide substrates, CVIM and CVLS, are significantly different and have been proposed to reflect a rate-limiting S_N2-like transition state with dissociative characteristics for CVIM, while, due to the absence of an isotope effect, CVLS was proposed to have a rate-limiting peptide conformational change. Potential of mean force quantum mechanical/molecular mechanical studies coupled with umbrella sampling techniques were performed to further probe this mechanistic dichotomy. We observe the experimentally proposed transition state (TS) for CVIM but find that CVLS has a symmetric S_N2 TS, which is also consistent with the absence of a ³H α -SKIE. These calculations demonstrate facile substrate-dependent alterations in the transition state structure catalyzed by FTase.

Protein farnesyltransferase (FTase) and protein geranylgeranyltransferase type I (GGTase I) have been extensively studied, due to their involvement in cancer and as potential targets for cancer treatment.¹ Both enzymes catalyze the posttranslational attachment of a prenyl group (FTase: 15-carbon farnesyl, GGTase I: 20-carbon geranylgeranyl) to a cysteine residue in a conserved Ca₁a₂X sequence at or near the C-terminus of a protein (see Figure 1). C refers to cysteine, a₁

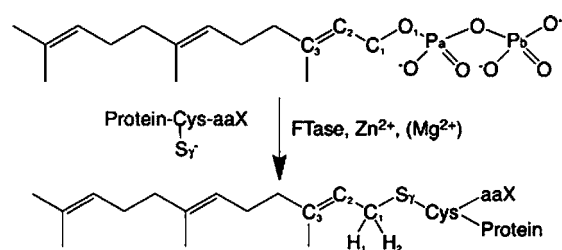


Figure 1. FTase catalyzed farnesylation. Important atoms are labeled.

is an amino acid with little sequence selectivity, a₂ is an aliphatic amino acid, and X typically corresponds to alanine, serine, methionine (for FTase), phenylalanine (for FTase and GGTase I), or leucine (for GGTase I).² This motif can be recognized and modified by FTase or GGTase I in the form of either a

protein, like Ras, or a short peptide. Prenylation is essential to the function of a variety of enzymes including multiple Ras subfamily members, enabling them to localize to the cell membrane to play roles in signal regulation. Therefore, inhibition of prenylation could be used in the treatment of certain types of cancers by affecting the function of mutated Ras enzymes (found in about 30% of human cancers³). Indeed, several FTase inhibitors have entered phase III clinical trials and have shown promise.⁴

FTase and GGTase I possess very similar overall structures: they share nearly identical α -subunits and highly homologous β -subunits. The binding pocket for their respective reactants, Ca₁a₂X and the corresponding isoprenoid diphosphate, are situated at the interface of two subunits, surrounded by the conserved residues, Lys164 α , His248 β (His219 β), Arg291 β (Arg263 β), Lys294 β (Lys266 β), and Tyr300 β (Tyr272 β) (residues in parentheses refer to those in GGTase I throughout). Both enzymes require a zinc ion for catalytic activity. In their activated forms, zinc is coordinated to Cys1p (targeted Ca₁a₂X cysteine), Asp297 β (Asp269 β), Cys299 β (Cys271 β), and His362 β (His321 β), forming a tetrahedral cluster. Fierke and co-workers determined that Cys1p is a thiolate rather than a thiol based on pH dependence studies.⁵ In the crystal structures (1QBQ⁶ and 1TN8⁷ of 2 Å resolution), the Zn²⁺-S_{Cys299 β} distance is 0.1–0.2 Å shorter than the Zn²⁺-S_{Cys1p} distance, suggesting weaker coordination between the zinc and peptide cysteine. This weak coordination has been proposed to enhance the nucleophilicity of the sulfur atom of the target cysteine that is essential for the S_N2-like reaction.⁸ In the crystal structure of FTase complexed with the prenylated K-Ras product (PDB code 1KZP,⁹ 2.10 Å resolution), the Zn²⁺-S_{Cys1p} distance increases to 2.66 Å, providing additional support for this hypothesis.⁹ FTase also requires a magnesium ion for optimal reactivity, but the position of this ion has not been observed crystallographically. Mutagenesis studies suggest that Asp352 β coordinates magnesium.^{10,11} Interestingly, in GGTase I, which is not activated by magnesium, this residue is a lysine (Lys311 β) that has been proposed to functionally substitute for the Mg²⁺ ion.¹² Although farnesyl diphosphate (FPP) can exist as a fully deprotonated form or its monoprotonated form (FPPH) at physiological pH in the absence of magnesium,⁵ previous computational work suggested the FPPH form, with

Received: October 13, 2011

Published: December 28, 2011

one of the β -diphosphate oxygen atoms protonated, is preferred in this situation.¹³

An important feature of the ternary (FTase/FPP/Ca₁a₂X) resting state (RS) is a C₁–S _{γ} distance of over 7 Å. A conformational transition exclusively associated with FPP and the peptide substrate (not the enzyme) is required to close this gap prior to the chemical step^{9,10,13,14} (see Figure S1). The catalytic mechanism of the subsequent chemical step has been debated for a number of years. Evidence supporting both an S_N2-like mechanism (associative) and an S_N1-like mechanism (dissociative) has been put forward.^{15–17} However, recent experimental and computational studies strongly support an associative mechanism with dissociative characteristics.^{18,19} Additionally, research carried out in the Fierke lab revealed that substrate recognition by FTase is context dependent,²⁰ which illustrated that the identity of both X and a₂ play important roles in the catalytic efficiency. Moreover, in ³H α -secondary kinetic isotope effect (α -SKIE) experiments, a value of near unity (1.00 ± 0.04) was obtained for FTase catalyzing single turnover farnesylation of GCVLS while a significantly larger value (1.154 ± 0.006) was observed for FTase with the peptide TKCVIF.¹⁹ This difference was attributed to the presence of different rate-determining steps (RDSs), which were proposed to involve the chemical step for FTase/TKCVIF, while for FTase/GCVLS the physical or conformational change step was hypothesized to be rate-limiting. This is an interesting observation given that the free energy of activation for farnesylation catalyzed by FTase is ~20 kcal/mol and the conformational change is localized to the substrates and not the enzyme (see Figure S1), which suggests that the peptide conformational transition is very highly constrained in FTase/GCVLS. Herein we describe studies testing this observation.

When we investigated the conformational transition step using potential of mean force (PMF) studies for the FTase/CVIM and FTase/CVLM complexes with classical molecular dynamics (MD) simulations, only small differences in the free energy barriers of the conformational step were observed.¹³ This result indicated that a single change in the a₂ position of the Ca₁a₂X motif was unable to alter the RDS but did not address the situation where both X and a₂ were altered in the Ca₁a₂X motif. Moreover, the details of the chemical step following the conformational step were not studied. Hence, a quantum mechanical molecular mechanical (QM/MM) study was carried out in order to further elucidate both the conformational and chemical steps in FTase catalysis. In fact, although MD simulations carried out at the molecular mechanical (MM) level provided useful insights into the conformational step in FTase,^{13,21–23} theoretical studies at the QM/MM²⁴ level add an extra dimension.^{18,25,26} In particular, in the chemical step where bond breaking and forming are important, classical MM theory is inappropriate. The self-consistent-charge density-functional tight-binding (SCC-DFTB) method has become a popular choice in QM/MM simulations, especially in zinc metalloenzymes and those cases involving phosphate reactions.^{27–31} Moreover, the SCC-DFTB/MM method has been extensively tested and good accuracy has been reported.^{32–35} Furthermore, a recent SCC-DFTB based computational study by Roitberg and co-workers elucidated the catalytic mechanism and successfully reproduced the experimental KIE in *Trypanosoma cruzi* trans-sialidase.³⁶ Hence, SCC-DFTB was adopted to study the farnesylation

reaction catalyzed by both FTase/FPPH/CVIM (CVIM) and FTase/FPPH/CVLS (CVLS) complexes.

The acetyl-capped CVIM peptide represents the Ca₁a₂X motif of human K-Ras, the mutant of which is usually found in lung cancers. After equilibration with the QM/MM potential, a steered MD (SMD) simulation was conducted to propagate the trajectory along the reaction coordinate (RC) defined as the distance between the two reacting atoms: the C₁ carbon from FPPH and the S _{γ} from the peptide cysteine. Including the C₁–O₁ bond into the RC results in an unphysical dissociative pathway, and this same observation has been reported by Klein and co-workers¹⁸ (see SI for further comparisons between this work and ref 18). The RC ranged from 1.8 to 8.0 Å (6.2 Å in total) that covered both the conformational and chemical steps. The free energy curve yielded a C₁–S _{γ} distance of approximately 2.6 Å at the transition state (TS). This value is slightly longer than the 2.4–2.5 Å TS C–S distance found in a model S_N2 reaction studied at the MP2/6-31+G**//MP2-6-31+G* level of theory.³⁷ Subsequently, a set of umbrella sampling (US) simulations were carried out along the RC and WHAM³⁸ was employed to construct the free energy profile. Our results indicate that farnesylation by CVIM, indeed, involves an associative mechanism with dissociative character. The highest free energy barrier is 20.6 kcal/mol, which corresponds to the chemical step and is in excellent agreement with experimental results^{16,19} (see Figure 2). Moreover, the

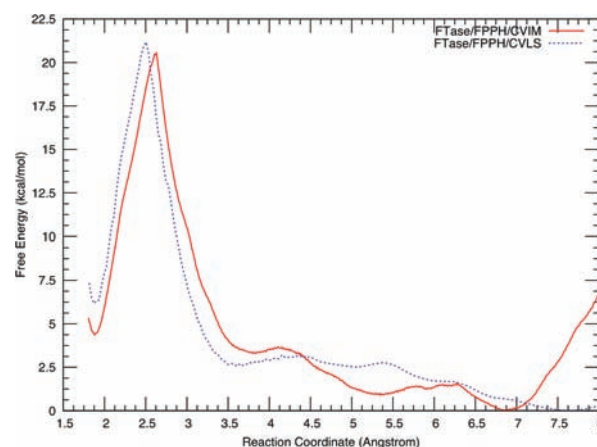


Figure 2. Free energy profile of farnesylation catalyzed by FTase/FPPH/CVIM (red) and FTase/FPPH/CVLS (blue).

conformational transition along the reaction coordinate matches our previous MM study, with a 6.9 Å (7.2 Å from MM) RS, 5.3 Å (5.0 Å from MM) intermediate, and an ~1.0 kcal/mol energy barrier separating them.¹³ Importantly, another shallow intermediate state was identified between the 5.3 Å intermediate and the TS at around 3.9 Å, where the O₁, C₁, and S _{γ} atoms are aligned in a linear arrangement which is favorable for S_N2 displacement. At the TS (see Figure 3), the H₁–H₂–C₁–C₂ dihedral is 169°, puckered slightly from a planar arrangement; moreover, the sign of this dihedral changes beyond this point, strengthening the point that the TS has been reached. The d_{C₁–S _{γ}} distance is 2.63 Å, the C₁–O₁ bond is breaking and reaches 2.3–2.5 Å, while the Zn–S _{γ} distance shows a 0.05 Å increase, indicating a weaker coordination between zinc and peptide cysteine. Beyond the TS, the d_{C₁–S _{γ}} continues decreasing, the d_{C₁–O₁} distance keeps quickly increasing until around 3.5 Å, and the d_{Zn–S _{γ}} reaches 2.50–

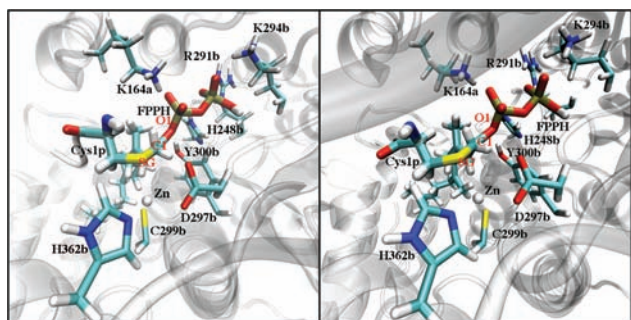


Figure 3. TS active site snapshots of FTase/FPPH/CVIM (left) and FTase/FPPH/CVLS (right). Also see Figure S4.

2.55 Å in the product state. Throughout the entire reaction, key residues in the FPPH binding pocket, such as Lys164 α , His248 β , Arg291 β , Lys294 β , and Tyr300 β , all form stabilizing hydrogen bonds with the diphosphate-leaving group. The Zn(II) coordination site is maintained during the process, but the $d_{\text{Zn-S}\gamma}$ increases from ~ 2.35 to ~ 2.50 Å. Such an increase has also been discovered in the crystal structures reported by Long, et al.⁹ Additionally, Fierke and co-workers have proposed that a weak zinc–sulfur coordination enhances the nucleophilicity of S γ .⁸ Qualitatively, our observed increase of the $d_{\text{Zn-S}\gamma}$ distance supports the notion of the enhanced nucleophilicity at S γ .

The acetyl-capped CVLS peptide has the same Ca₁a₂X sequence as H-Ras, whose malfunction has been implicated in bladder cancers. The PMF study was carried out on both the physical step (at the MM level) and chemical step (at the QM/MM level). The free energy barrier associated with the conformational transition is ~ 2.8 kcal/mol. This value is of the same order of magnitude as observed for CVIM (~ 1.0 kcal/mol, at both the QM/MM and MM level), FTase/FPPH/CVLM (~ 2.5 kcal/mol), and Y β 300F/FPPH/CVIM (~ 1.4 kcal/mol). Obviously, such a small barrier is insufficient to cause the predicted RDS change. In fact, the experimental free energy barrier height for FTase/GCVLS is 20 kcal/mol (in the absence of Mg²⁺), while our QM/MM results gave a 21.3 kcal/mol free energy barrier, not for the physical step, but for the chemical step. Hence, another hypothesis needs to be developed to explain the observed near unity ³H α -SKIE measurement. However, the possibility that an upstream sequence (TK) also influences α -SKIE cannot be excluded and is being explored.

α -SKIEs are useful in distinguishing S_N1 and S_N2 reaction types because they are sensitive to bond hybridization changes and the resultant changes in zero-point energies (ZPEs). In a typical symmetrical S_N2 reaction, $k_{\text{H}}/k_{\text{T}}$ tends to be smaller and near unity ($\sim 1.00 \pm 0.06$), while the values observed for S_N1 reactions are ~ 1.1 – 1.2 .³⁹ In the CVLS chemistry step, $d_{\text{C1-S}\gamma}$ at the TS is 2.51 Å (see Figure 3), which is 0.12 Å shorter than what was found for CVIM and much closer to the value reported by Gronert et al. in their study of a related S_N2 reaction involving sulfur at the MP2/6-31+G**//MP2-6-31+G* level of theory.³⁷ At the TS, the O₁, C₁ of FPPH, and S γ of Cys1p are nearly colinear with only C₁ being slightly out of plane and the C₁–O₁ bond is more constrained, reaching only 1.8–2.0 Å, and continues to slowly increase beyond the TS. The H₁–H₂–C₁–C₂ dihedral is nearly planar in the TS with a value of 179.6°, which decreases rapidly on both sides of this peak (see Figure S2). Hence, the structural evidence

supports a more typical S_N2-like TS. During this reaction, the binding pocket amino acids do not experience large fluctuations, further confirming that an enzyme based conformational change that is large enough to alter the RDS is unlikely. The Zn(II) coordination site is maintained during the process with the $d_{\text{Zn-S}\gamma}$ increasing by about 0.1 Å.

As mentioned previously, the most important factor in the differences between k_{H} and k_{T} is the ZPE. In light of this, we performed a QM optimization followed by frequency analysis with the M06-2X/6-31+G** level of theory,^{40,41} on the QM part of the system abstracted from the prenylation TSs for CVIM and CVLS, respectively. Subsequently, we calculated the $\Delta\Delta E_{\text{ZPE}}$ for both CVLS and CVIM, based on $\Delta\Delta E_{\text{ZPE}} = \Delta E_{\text{ZPE}}^{\text{T}} - \Delta E_{\text{ZPE}}^{\text{H}}$, where $\Delta E_{\text{ZPE}} = E_{\text{ZPE}}^{\text{TS}} - E_{\text{ZPE}}^{\text{GS}}$ for both H and T. An ~ 0.13 kcal/mol difference of $\Delta\Delta E_{\text{ZPE}}$ was identified, with the CVIM complex possessing the larger $\Delta\Delta E_{\text{ZPE}}$ (0.14 ± 0.02 kcal/mol) and the CVLS complex having a $\Delta\Delta E_{\text{ZPE}}$ near zero (0.01 ± 0.01 kcal/mol). This strengthens our proposal that the CVLS peptide prefers an S_N2-like reaction pathway. Moreover, these results are qualitatively in accordance with the experimental trends (an approximate 0.085 kcal/mol $\Delta\Delta G$ for FTase/TKCVIF in the absence of Mg²⁺; see Supporting Information (SI)). More importantly, it demonstrates that the slight differences observed in the reaction mechanisms reflect the experimentally observed $k_{\text{H}}/k_{\text{T}}$ differences. We also qualitatively monitored charge variation through the reaction course of CVLS and CVIM prenylation using Mulliken charges. The summation of the charges on the C₁, C₂, and C₃ atoms (comprising an allyl-like group) of the farnesyl group are of particular interest, because in a dissociative reaction pathway the developing partial positive charge would be delocalized across this allyl fragment, while in a pure S_N2 reaction a less positive charge would be developed in the TS. For CVIM +0.032q is delocalized into the allyl moiety, which is 10 times smaller (+0.003q) in CVLS. This result strengthens our conclusion that the reaction mechanism for CVLS is a typical S_N2 reaction (synchronous A_ND_N) and an associative mechanism with dissociative characteristics (dissociative A_ND_N) for CVLM. Providing further support for our results is the agreement between the computed and experimental free energies of activation. The free energy barrier for the CVLS peptide was computed to be 21.3 kcal/mol, in excellent agreement with the 20.0 kcal/mol experimental value.¹⁶ In addition, the computed free energy barrier difference between CVLS and CVIM is approximately 0.8 kcal/mol, which also is in agreement with the experimentally observed ~ 0.5 kcal/mol difference (although the experimental result is measured in the presence of Mg²⁺).²⁰

The residues in the a₂ and X positions in the Ca₁a₂X motif have been shown to strongly affect substrate selection, with selection of the side chain at the a₂ position being dependent on both hydrophobicity and volume.²⁰ The different behavior of the a₂ residue between CVIM and CVLS was monitored via a modified Ramachandran plot. In this plot, we monitored the a₂ residue in terms of Ψ – Φ torsion angles throughout the chemical step (see Figure S3), for both complexes. In CVIM, the Ile3p remained in the α -region, while, for CVLS, Leu3p fluctuates in the transition region connecting the α - and β -regions. We propose that in the CVLS system the peptide sacrifices its conformational stability to facilitate bringing the two substrates together, while for CVIM the peptide remains in the α -region, so the energetic cost of the conformational step is mainly attributed to the rotation of FPPH. Preliminary results

show that, for CVLM, the Leu3p also remains in the α -region (see Figure S3). Therefore, it appears that the differential a_2 behavior observed in the CVLS and CVIM (CVLM) complexes cannot be fully attributed to a single change at the a_2 position but to a double change at the a_2 and X positions, in support of the context-dependent substrate recognition hypothesis of Fierke and co-workers.²⁰

In conclusion, we have put forth an alternative proposal for FTase catalysis that involves differential S_{N1}/S_{N2} -like behaviors as a function of the peptide to be farnesylated. Thus, FTase activity appears to be fully governed by the chemical step with the conformational step only playing a modest role. Furthermore, the small energetic differences between the S_{N1} and S_{N2} transition states in the enzymes allow substrate dependent alteration in the transition state structure.

■ ASSOCIATED CONTENT

● Supporting Information

Methods and computation details, short trajectory movies, and key structures. This material is available free of charge via the Internet at <http://pubs.acs.org>.

■ AUTHOR INFORMATION

Corresponding Author

merz@qtp.ufl.edu

■ ACKNOWLEDGMENTS

The authors thank Dr. Adrian E. Roitberg, Dr. Nicole A. Horenstein, and Dr. June Pais for helpful discussions and the NIH for financial support of this project through grants (GM044974) to K.M.M. and (GM040602) for C.A.F. We also thank Dr. Qiang Cui for sharing phosphorous parameters for SCC-DFTB.

■ REFERENCES

- (1) Zhang, F. L.; Casey, P. J. *Annu. Rev. Biochem.* **1996**, *65*, 241–269.
- (2) Lamphear, C. L.; Zverina, E. A.; Houglund, J. L.; Fierke, C. A. *The Enzymes-Protein Prenylation/Part A* **2011**, *29*, 207–234.
- (3) Cox, A. D. *Drugs* **2001**, *61*, 723–732.
- (4) Doll, R. J.; Kirschmeier, P.; Bishop, W. R. *Curr. Opin. Drug Discovery Dev.* **2004**, *7*, 478–486.
- (5) Saderholm, M. J.; Hightower, K. E.; Fierke, C. A. *Biochemistry* **2000**, *39*, 12398–12405.
- (6) Strickland, C. L.; Windsor, W. T.; Syto, R.; Wang, L.; Bond, R.; Wu, Z.; Schwartz, J.; Le, H. V.; Beese, L. S.; Weber, P. C. *Biochemistry* **1998**, *37*, 16601–16611.
- (7) Reid, T. S.; Terry, K. L.; Casey, P. J.; Beese, L. S. *J. Mol. Biol.* **2004**, *343*, 417–433.
- (8) Tobin, D. A.; Pickett, J. S.; Hartman, H. L.; Fierke, C. A.; Penner-Hahn, J. E. *J. Am. Chem. Soc.* **2003**, *125*, 9962–9969.
- (9) Long, S. B.; Casey, P. J.; Beese, L. S. *Nature* **2002**, *419*, 645–650.
- (10) Pickett, J. S.; Bowers, K. E.; Fierke, C. A. *J. Biol. Chem.* **2003**, *278*, 51243–51250.
- (11) Yang, Y.; Chakravorty, D. K.; Merz, K. M. *Biochemistry* **2010**, *49*, 9658–9666.
- (12) Hartman, H. L.; Bowers, K. E.; Fierke, C. A. *J. Biol. Chem.* **2004**, *279*, 30546–30553.
- (13) Cui, G.; Merz, K. M. Jr. *Biochemistry* **2007**, *46*, 12375–12381.
- (14) Long, S. B.; Hancock, P. J.; Kral, A. M.; Hellinga, H. W.; Beese, L. S. *Proc. Natl. Acad. Sci. U.S.A.* **2001**, *98*, 12948–12953.
- (15) Dolence, J. M.; Poulter, C. D. *Proc. Natl. Acad. Sci. U.S.A.* **1995**, *92*, 5008–5011.
- (16) Huang, C. C.; Hightower, K. E.; Fierke, C. A. *Biochemistry* **2000**, *39*, 2593–2602.
- (17) Edelstein, R. L.; Weller, V. A.; Distefano, M. D.; Tung, J. S. *J. Org. Chem.* **1998**, *63*, 5298–5299.
- (18) Ho, M.-H.; Vivo, M. D.; Peraro, M. D.; Klein, M. L. *J. Chem. Theory Comput.* **2009**, *5*, 1657–1666.
- (19) Pais, J. E.; Bowers, K. E.; Fierke, C. A. *J. Am. Chem. Soc.* **2006**, *128*, 15086–15087.
- (20) Houglund, J. L.; Lamphear, C. L.; Scott, S. A.; Gibbs, R. A.; Fierke, C. A. *Biochemistry* **2009**, *48*, 1691–1701.
- (21) Cui, G.; Wang, B.; Merz, K. M. Jr. *Biochemistry* **2005**, *44*, 16513–16523.
- (22) Cui, G.; Li, X.; Merz, K. M. Jr. *Biochemistry* **2006**, *46*, 1303–1311.
- (23) Sousa, S. F.; Fernandes, P. A.; Ramos, M. J. *Bioorg. Med. Chem.* **2009**, *17*, 3369–3378.
- (24) Warshel, A.; Levitt, M. *J. Mol. Biol.* **1976**, *103*, 227–249.
- (25) Sousa, S. F.; Fernandes, P. A.; Ramos, M. J. *Chem.—Eur. J.* **2009**, *15*, 4243–4247.
- (26) Sousa, S. F.; Fernandes, P. A.; Ramos, M. J. *Proteins: Struct., Funct., Bioinf.* **2007**, *66*, 205–218.
- (27) Elstner, M.; Porezag, D.; Jungnickel, G.; Elsner, J.; Haugk, M.; Frauenheim, T.; Suhai, S.; Seifert, G. *Phys. Rev. B* **1998**, *58*, 7260–7268.
- (28) Elstner, M.; Cui, Q.; Muni, P.; Kaxiras, E.; Frauenheim, T.; Karplus, M. *J. Comput. Chem.* **2003**, *24*, 565–581.
- (29) Yang, Y.; Yu, H. B.; York, D.; Elstner, M.; Cui, Q. *J. Chem. Theory Comput.* **2008**, *4*, 2067–2084.
- (30) Moreira, N. H.; Dolgonos, G.; Aradi, B.; da Rosa, A. L.; Frauenheim, T. *J. Chem. Theory Comput.* **2009**, *5*, 605–614.
- (31) Elstner, M.; Gaus, M. G., M.; Cui, Q. *J. Chem. Theory Comput.* **2011**, *7*, 931–948.
- (32) Guo, H.; Guo, H. B.; Rao, N.; Xu, Q. *J. Am. Chem. Soc.* **2005**, *127*, 3191–3197.
- (33) Guo, H.; Xu, D.; Cui, G. *J. Am. Chem. Soc.* **2007**, *129*, 10814–10822.
- (34) Xu, D. G.; Guo, H. *J. Am. Chem. Soc.* **2009**, *131*, 9780–9788.
- (35) Xu, D. G.; Wu, S. S.; Guo, H. *J. Am. Chem. Soc.* **2010**, *132*, 17986–17988.
- (36) Pierdominici-Sottile, G.; Horenstein, N. A.; Roitberg, A. E. *Biochemistry* **2011**, *50*, 10150–10158.
- (37) Gronert, S.; Lee, J. M. *J. Org. Chem.* **1995**, *60*, 6731–6736.
- (38) Grossfield, A. *WHAM code*, 1.6d ed.
- (39) Purich, D. L.; Allison, R. D. *Handbook of Biochemical Kinetics*; Academic Press: San Diego, CA, 2000.
- (40) Truhlar, D. G.; Zhao, Y. *Theor. Chem. Acc.* **2008**, *120*, 215–241.
- (41) Truhlar, D. G.; Zhao, Y. *Acc. Chem. Res.* **2008**, *41*, 157–167.